

Charge storage in $\text{CeO}_2/\text{Si}/\text{CeO}_2/\text{Si}(111)$ structures by electrostatic force microscopy

J. T. Jones, P. M. Bridger, O. J. Marsh, and T. C. McGill^{a)}

Thomas J. Watson, Sr., Laboratory of Applied Physics, California Institute of Technology, Pasadena, California 91125

(Received 26 March 1999; accepted for publication 8 July 1999)

An electrostatic force microscope was used to write and image localized dots of charge in a double barrier $\text{CeO}_2/\text{Si}/\text{CeO}_2/\text{Si}(111)$ structure. By applying a relatively large tip voltage and reducing the tip to sample separation to 3–5 nm, charge dots 60–200 nm full width at half maximum of both positive and negative charge have been written. The total stored charge is found to be $Q = \pm(20\text{--}200)e$ per charge dot. These dots of charge are shown to be stable over periods of time greater than 24 h, with an initial charge decay time constant of $\tau \sim 9.5$ h followed by a period of much slower decay with $\tau > 24$ h. The dependence of dot size and total stored charge on various writing parameters such as tip writing bias, tip to sample separation, and write time is examined.

© 1999 American Institute of Physics. [S0003-6951(99)04035-8]

Cerium oxide (CeO_2) is an insulating material with a lattice mismatch of only 0.35% to silicon (Si) and an energy band gap of ~ 5.5 eV. This attractive set of properties has the potential to lead to a fully functional silicon heterojunction technology. A significant amount of work has been done examining the growth and characterization of CeO_2 crystals on Si,^{1–5} and the growth of single crystal Si on to CeO_2/Si heterostructures⁶ has been recently reported. Based on these promising results, a silicon resonant tunneling diode, an improved silicon-on-insulator technology, and stacked silicon electronics have all been proposed. A valuable and interesting addition to this array of technologies would be the capacity for integrated electrostatic data storage.

In this letter, we describe the localized charging and subsequent imaging of a double barrier $\text{CeO}_2/\text{Si}/\text{CeO}_2/\text{Si}(111)$ structure by electrostatic force microscopy (EFM).^{7–9} The controllable writing of both positive and negative localized dots of charge with long lifetimes is described and it is further shown that these charge dots may be rewritten and replaced by charge of the opposite sign through the application of an opposite charging bias. A simple analysis is presented to quantify the total amount of charge stored in each charge dot. The time evolution of these charge dots is studied, and charge decay time constants are extracted. Finally, a study is presented of various writing parameters such as tip bias, tip to sample separation, and write time on the size and total stored charge of the resultant charge dots.

Samples were produced from commercially available 3 in. Si(111) wafers, *n*-type with 3.0–4.3 Ω cm resistivity. After being subjected to a standard acetone, isopropyl alcohol, deionized water degrease in ultrasound, the wafer was etched in 50:1 HF solution until hydrophobic, rinsed in deionized water, and immediately introduced into vacuum. Electron beam evaporation was used to deposit material from an undoped Si charge and a 99.99% CeO_2 charge to grow the structures. Initially, a 200 Å Si buffer layer was grown and examined by (RHEED) reflection high-energy electron dif-

fraction to assure the characteristic (7×7) reconstruction was apparent, indicative of a clean Si surface ready for further growth. Cerium oxide thin films were grown at a wafer temperature of 550 °C, with chamber pressures ranging from 1×10^{-7} – 2×10^{-6} Torr due primarily to outgassing from the CeO_2 charge. Silicon thin films were also grown at a wafer temperature of 550 °C, with chamber pressures of 5×10^{-8} – 2×10^{-7} Torr. A double barrier structure, $\text{CeO}_2/\text{Si}/\text{CeO}_2/\text{Si}(111)$, was produced with symmetric 35 Å CeO_2 barriers and an intermediate 25 Å Si film. *In situ* RHEED was again used to monitor film growth and showed the CeO_2 barriers and intermediate Si film to be polycrystalline.

The EFM data were collected using a Digital Instruments Nanoscope IIIa controller and a Bioscope scanning probe microscope operating in tapping mode. To detect the electrostatic forces, a voltage is applied to commercially available cobalt coated tapping mode atomic force microscopy (AFM) tips which are scanned across the surface at a constant tip to sample separation. Phase differences induced by electrostatic forces on the oscillating tip during scanning are detected and provide a measurement of the local charge density. In all cases, topographical AFM images and electrostatic EFM images were recorded simultaneously.

By reducing the tip to sample separation and applying a large charging bias to the EFM tip, dots of both positive and negative charge can be written as shown in Fig. 1. Writing was performed by restricting the EFM tip to a 1 nm² area, bringing it to within 5 nm of the sample, and applying a charging bias of ± 10 V for 45 s. Subsequent imaging of the resultant charge dots was performed over a $1 \mu\text{m} \times 1 \mu\text{m}$ area by increasing the tip to sample distance to 30 nm and imaging at a tip bias of 1 V. No change in the topographical AFM image was detected, but positive and negative dots of charge 115 nm full width at half maximum (FWHM) are clearly visible in the EFM image. Application of a positive charging bias results in positive features in the subsequent EFM imaging at $V_{\text{EFM}} = 1$ V. It was further shown that by repeating the write sequence at the same location with a charging volt-

^{a)}Electronic mail: tcm@ssdp.caltech.edu

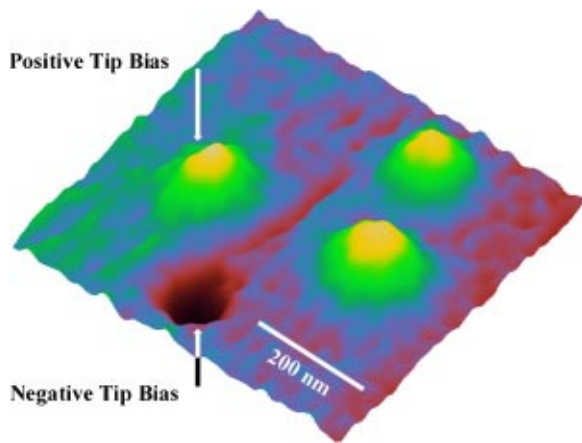


FIG. 1. A square array of 115 nm FWHM charge dots, 3 positive and 1 negative, written with an EFM to a CeO₂/Si/CeO₂/Si heterostructure. Application of a positive tip bias during writing results in positive features in the EFM image at V_{EFM}=1 V. Total charge on the dots is computed to be Q=±42e. No topographical changes are detected by AFM after writing, but the charge dots are clearly visible in the EFM image. Charge dots of both positive and negative charge have also been rewritten over top one another by application of an opposite writing voltage.

age of opposite polarity, a charge dot could be effectively rewritten with one of an opposite charge.

To compute the total stored charge, Q, we first use an electrostatic analysis in similar fashion to Ref. 10 to compute the localized stored charge, q, from a frequency shift, Δf. When the detected phase difference, Δφ, is very small, the relationship between Δφ and Δf is nearly linear and is found to be Δf~3.5Δφ Hz/deg for our tip. The frequency shift, Δf, is related to the gradient of the force by the expression Δf=-f₀f'(z₀)/(2k), where z₀=30 nm is the tip to sample separation during imaging, f₀=59.8 kHz is the resonant frequency of the tip, and k=3 N/m is the estimated spring constant of the tip. The force the tip feels under an applied direct current (dc) bias will be due to charge-charge interactions and is given by

$$F(z) = \frac{1}{[z + (2d_{\text{CeO}_2}/\epsilon_{\text{CeO}_2}) + (d_{\text{Si}}/\epsilon_{\text{Si}})]^2} \times \left(-\frac{d_{\text{CeO}_2}^2 q^2}{\epsilon_{\text{CeO}_2}^2 \epsilon_0 a} + \frac{2d_{\text{CeO}_2} q V_{\text{EFM}}}{\epsilon_{\text{CeO}_2}} + \frac{\epsilon_0 a V_{\text{EFM}}^2}{2} \right), \quad (1)$$

where z is again the tip to sample separation, d and ε are the thickness and dielectric constant of the CeO₂ and Si films, as indexed, V_{EFM} is the bias applied to the tip, and a is the area of the charged region. Simple modeling predicts the EFM image of a localized charge to be 56 nm FWHM, with an area a=2450 nm². The first term in the bracket in Eq. (1) is

TABLE I. A summary of the structures studied to examine the effect of the lower CeO₂ barrier on charge retention time τ.

Sample	CeO ₂ (Å)	Si (Å)	CeO ₂ (Å)	Si buffer (Å)	τ (h)
CE-41	35	25	35	200	9.8
CE-44	35	25	15	200	0.3
CE-43	35	200	0.2

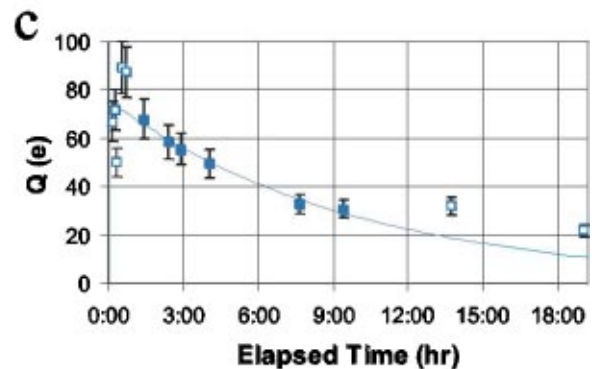
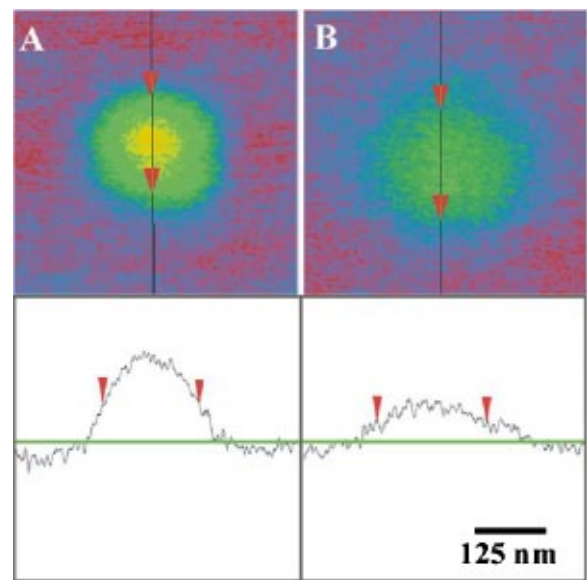


FIG. 2. Before (a) and after (b) images of a charge dot over time illustrating the spreading and net decrease in total charge Q. A plot of the time evolution of Q in a separate dot (c) exhibits an initial decay with τ~9.5 h (fit line), followed by a period of much slower decay with τ>24 h.

found to be negligibly small,⁷ and the last term provides a constant background independent of the charge. Using only the middle term and the values given above, an approximation to the localized stored charge is then given by q=43Δφ e/deg. Computing the total stored charge in our

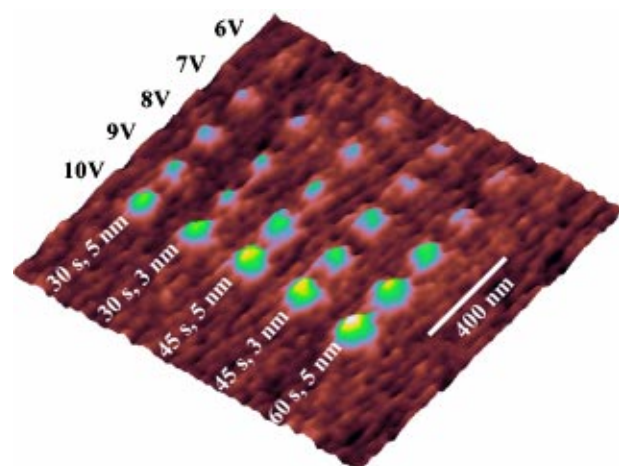


FIG. 3. An EFM image of an array of dots written at different writing voltages, tip to sample separations, and writing times as labeled. Local charge density, q, and dot size are strongly dependent on writing voltage and time, and more weakly dependent on tip to sample separation.

EFM images of area A , we find $Q = q(A/a)e$. For the dots in Fig. 1, $\Delta\phi = \pm 0.23^\circ$ over an area of $A = 1 \times 10^5 \text{ nm}^2$, we compute $Q = \pm 42e$.

To examine the time evolution of stored charge in our system, single charge dots were written and monitored over time. In all cases, the general trend was for a slow leakage of charge accompanied by an increase in FWHM of the charge dot, as shown in Figs. 2(a) and 2(b). To estimate the lifetime associated with the stored charge, a single charge dot was written and continuously monitored over several days. After writing at $V_{\text{EFM}} = 10 \text{ V}$, $z = 3 \text{ nm}$, and $t = 60 \text{ s}$, the resultant charge dot was continuously imaged at $V_{\text{EFM}} = 1 \text{ V}$ and $z = 30 \text{ nm}$ at a read speed of 21 reads/h for the first 4 h, after which imaging was performed intermittently for the remainder of the experiment. A plot of the total stored charge, Q , is shown in Fig. 2(c). There is an initial period of charge settling and reorganization during which it is difficult to reliably extract charge dot profiles. After this settling period and over the first 10 h, an exponential fit to the charge decay exhibits a time constant $\tau \sim 9.5 \text{ h}$, after which the rate of decay slows down considerably to $\tau > 24 \text{ h}$. After a period of $t > 40 \text{ h}$; the stored charge was no longer detectable by our instrument. As the charge lifetime is found to be invariant to whether the tip was continuously or intermittently engaged, as exhibited by the uniform decay up until $t = 10 \text{ h}$ in Fig. 2(b), charge leakage to the EFM tip is ruled out and the decay mechanism is determined to be tunneling into the Si substrate.

To determine the effect of the lower CeO_2 barrier on charge retention time, two additional samples were studied: a single barrier control sample consisting of 35 \AA CeO_2 atop the crystalline silicon buffer layer, and a double barrier structure with a 35 \AA CeO_2 upper barrier, a 25 \AA Si well, and a reduced 15 \AA CeO_2 lower barrier, as shown in Table I. In both CE-43 and CE-44 it was found that significantly less charge was stored under standard write conditions of $V_{\text{EFM}} = 10 \text{ V}$, $z = 3 \text{ nm}$, and $t = 60 \text{ s}$, and charge decay time constants were much shorter. The control sample, CE-43, was found to have a charge decay time constant of $\tau \sim 0.2 \text{ h}$, and the reduced barrier sample, CE-44, was found to have a charge decay time constant of $\tau \sim 0.3 \text{ h}$. These results clearly show that the lower CeO_2 barrier is serving as an inhibitor to the primary decay mechanism which is concluded to be tunneling into the Si substrate. Furthermore, the ability to store charge in the control sample indicates that charge is being stored at crystalline defects within the upper CeO_2 barrier or at the upper CeO_2/Si interface, ruling out the polycrystalline Si well as a potential storage site.

To examine the effects of writing parameters on charge dot size and total stored charge, an array of positive charge

dots was written at various EFM tip biases, tip to sample distances, and write times as shown in Fig. 3. Line scans were taken across the low pass filtered image to extract charge dot sizes and local charge densities, q . It is found in general that both the size and q of the charge dots scale linearly with the same slope in relation to the various writing parameters. From a nominal writing parameter start point of $V_{\text{EFM}} = 10 \text{ V}$, $t = 60 \text{ s}$, and $z = 5 \text{ nm}$, it is found that the size and q of a charge dot may be expected to decrease 10% for each 0.5 V decrease in V_{EFM} , decrease 10% for each 10 s decrease in t , and increase 10% for a 2 nm decrease in z .

In conclusion, an EFM was used to write and image localized dots of charge in a double barrier $\text{CeO}_2/\text{Si}/\text{CeO}_2/\text{Si}(111)$ structure. By applying relatively large tip voltages of $V_{\text{EFM}} = \pm(6-10) \text{ V}$ and reducing the tip to sample separation to $z = 3-5 \text{ nm}$, charge dots 60–200 nm FWHM of both positive and negative charge have been written. The total stored charge is found to be $Q = \pm(20-200)e$ per charge dot. These charge dots are shown to be stable over periods of time greater than a day, with an initial charge decay time constant of $\tau \sim 9.5 \text{ h}$ followed by a period of much slower decay with $\tau > 24 \text{ h}$. The dependence of charge dot size and total stored charge on various writing parameters such as tip bias, tip to sample separation, and write time has been examined and linear dependencies extracted.

This work was supported by the Defense Advanced Research Project Agency, and monitored by the Air Force Office of Scientific Research under Grant No. F49620-96-1-0021.

- ¹T. Inoue, Y. Yamamoto, S. Koyama, S. Suzuki, and Y. Ueda, *Appl. Phys. Lett.* **56**, 1332 (1990).
- ²L. Luo, X. Wu, R. Dye, R. Muenchansen, S. Foltyn, Y. Coulter, C. Maggiore, and T. Inoue, *Appl. Phys. Lett.* **59**, 2043 (1991).
- ³T. Inoue, Y. Yamamoto, M. Satoh, A. Ide, and S. Katsumata, *Thin Solid Films* **281-282**, 24 (1996).
- ⁴T. Chikyow, S. Bedair, L. Tye, and N. El-Masry, *Appl. Phys. Lett.* **65**, 1030 (1994).
- ⁵S. Yaegashi, T. Kurihara, H. Hoshi, and H. Segawa, *Jpn. J. Appl. Phys.*, Part 1 **33**, 270 (1994).
- ⁶J. Jones, E. Croke, C. Garland, O. Marsh, and T. McGill, *J. Vac. Sci. Technol. B* **16**, 2686 (1998).
- ⁷D. Sarid, *Scanning Force Microscopy* (Oxford University Press, New York, 1991).
- ⁸W. Nabhan, B. Equer, A. Broniatowski, and G. DeRosny, *Rev. Sci. Instrum.* **68**, 3108 (1997).
- ⁹M. Nonnenmacher, M. P. O'Boyle, and H. K. Wickramasinghe, *Appl. Phys. Lett.* **58**, 2921 (1991).
- ¹⁰D. Schaadt, E. Yu, S. Sankar, and A. Berkowitz, *Appl. Phys. Lett.* **74**, 472 (1999).